

Large-scale profiling of protein palmitoylation in mammalian cells

Brent R Martin & Benjamin F Cravatt

S-palmitoylation is a pervasive post-translational modification required for the trafficking, compartmentalization and membrane tethering of many proteins. We demonstrate that the commercially available compound 17-octadecynoic acid (17-ODYA) can serve as a bioorthogonal, click chemistry probe for *in situ* labeling, identification and verification of palmitoylated proteins in human cells. We identified ~125 predicted palmitoylated proteins, including G proteins, receptors and a family of uncharacterized hydrolases whose plasma membrane localization depends on palmitoylation.

S-palmitoylation is a reversible covalent post-translational attachment of fatty acids on cysteines that mediates association of diverse proteins with membranes via a labile acyl-thioester linkage¹. Many proteins have been identified as targets of palmitoylation, most notably G proteins, which are often palmitoylated next to prenylation or myristoylation sites. Other diverse classes of palmitoylated proteins include ion channels, receptors, cytoskeletal proteins and kinases.

Protein palmitoylation has historically been detected by metabolic incorporation of radiolabeled palmitate followed by immunological precipitation. This classical approach is tedious owing to lengthy film exposure times and the lack of any straightforward means to enrich and identify radiolabeled proteins. Alternatively, selective thioester hydrolysis and covalent tagging can be used to capture sites of palmitoylation in a method termed acyl-biotin exchange (ABE)². Coupling this approach to mass spectrometry provided the first global profile of palmitoylated proteins in *Saccharomyces cerevisiae*, identifying nearly 50 palmitoylation targets. The ABE method, however, requires complete blockage of all reduced cysteines to eliminate false positives, as well as highly efficient thioester hydrolysis and disulfide-exchange reactions to label and identify palmitoylated proteins. Coupled with the inherent background observed with streptavidin bead enrichments, these factors resulted in nearly one-third of the identified proteins being designated as false positives². Despite this initial promising work, large-scale identification of palmitoylated proteins from higher eukaryotic organisms, such as mammals, has yet to be reported, and we

accordingly still lack an understanding of the full extent and purpose of this post-translational modification in cell biology.

Several groups have recently reported the use of azido-fatty acids or azido-acyl coenzyme A (CoA) as probes for protein myristoylation and/or palmitoylation^{3–6}. Myristoylation describes the irreversible co-translational modification of the N-terminal residue (typically glycine) of proteins by myristoyl-CoA via an amide linkage. After reaction with biotin-linked phosphines or alkynes by the Staudinger ligation and copper (I)-catalyzed azide-alkyne cycloaddition (click chemistry), respectively, probe-modified proteins can be detected by avidin-horseradish peroxidase blotting. These reports demonstrated the utility of this approach for rapid detection of acylated proteins but stopped short of applying these probes for the global enrichment and identification of fatty-acylated proteins from native biological systems.

Building on these past studies, we describe here a simple and robust method for the global identification of palmitoylated proteins from human Jurkat T cells using the commercially available palmitic acid analog 17-octadecynoic acid (17-ODYA)⁷. For decades, 17-ODYA has been used as a ω -hydroxylase inhibitor for *in vitro* and *in vivo* inhibition of cytochrome P450 metabolism of fatty acids. We now describe the application of 17-ODYA as a metabolically incorporated biorthogonal probe for profiling endogenous protein targets of palmitoylation (Fig. 1a and

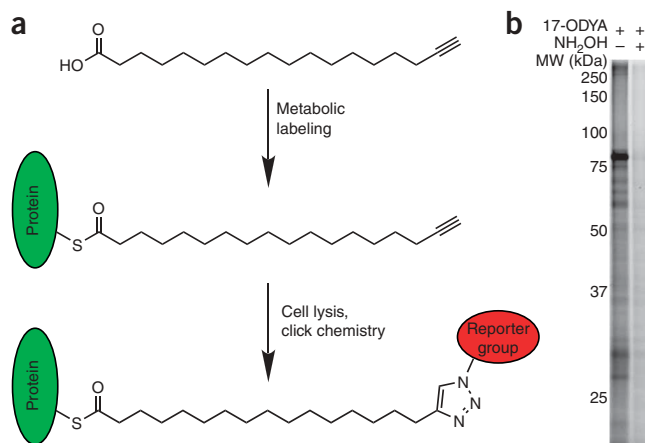


Figure 1 | The 17-ODYA labeling and detection of palmitoylated proteins. (a) Schematic of 17-ODYA labeling. Cultured cells are metabolically labeled with 17-ODYA and the lysates are then reacted with rhodamine-azide or biotin-azide for gel-based or LC-MS-based characterization of palmitoylated proteins. (b) Profile of palmitoylated proteins in the membrane fraction of Jurkat T cells incubated with 25 μ M 17-ODYA for 8 h. As a control, half of the sample was boiled in 2.5% hydroxylamine (NH_2OH) for 5 min to hydrolyze thioesters and remove 17-ODYA labeling.

The Skaggs Institute of Chemical Biology and Department of Chemical Physiology, The Scripps Research Institute, 10550 N. Torrey Pines Road, La Jolla, California 92037, USA. Correspondence should be addressed to B.F.C. (cravatt@scripps.edu).

RECEIVED 26 SEPTEMBER 2008; ACCEPTED 8 DECEMBER 2008; PUBLISHED ONLINE 11 JANUARY 2009; DOI:10.1038/NMETH.1293

Supplementary Methods online). We detected octadecynoylated proteins via the Cu(I)-catalyzed azide-alkyne [3 + 2] cycloaddition reaction (click chemistry) to commercially available rhodamine-azide or biotin-azide reporter groups⁸. We observed optimal metabolic labeling after incubation with 25 μ M of 17-ODYA for 6 h or longer (Supplementary Figs. 1 and 2 online), and labeled proteins were restricted to the membrane fraction (Supplementary Fig. 3 online). Nearly all detectable labeling was hydroxylamine-sensitive, signifying S-acylation is the predominant mode of protein modification by 17-ODYA (Fig. 1b).

To identify the targets of palmitoylation, we reacted membrane fractions from 17-ODYA-labeled Jurkat T cells with biotin-azide and enriched them for proteomic analysis by the multidimensional protein identification technology (MudPIT)⁹ (Table 1). In our first study ($n = 6$ per group), we compared 17-ODYA-treated cells to cells treated with an equal concentration of palmitic acid. In a second study ($n = 5$ per group), we labeled cells with 17-ODYA and

treated half of the sample with pH-neutral hydroxylamine to cleave 17-ODYA-protein thioester linkages. We estimated protein amounts in each sample by spectral counting, which sums the number of tandem mass spectrometry spectra assigned to a specific protein and is highly correlated with protein abundance¹⁰. We applied stringent thresholds to define predicted palmitoylated proteins as targets that appeared in either 17-ODYA dataset with (i) an average spectral count value ≥ 5 , (ii) signal in at least three replicate samples and (iii) spectral count ratios of ≥ 5 for 17-ODYA-treated versus corresponding control samples (Supplementary Table 1 online). In total, these two datasets led to the classification of 125 high-confidence predicted palmitoylated proteins. Lowering the spectral count threshold to include proteins with an average spectral count value between 2 and 5 resulted in the identification of an additional ~ 200 predicted palmitoylated proteins, which we designated as medium-confidence targets (Supplementary Table 2 online).

Table 1 | Spectral counts for the top 35 high-confidence palmitoylated proteins

Protein name	Protein description	Experiment 1 ($n = 6$)		Experiment 2 ($n = 5$)	
		17-ODYA	Palmitate	17-ODYA	Hydroxylamine
CANX	Calnexin	95 \pm 11	11 \pm 2	122 \pm 30	2 \pm 1
HLA-A, HLA-B, HLA-C	HLA class I histocompatibility antigen	68 \pm 10	13 \pm 6	68 \pm 12	0 \pm 0
LCK ^a	Proto-oncogene tyrosine-protein kinase LCK	75 \pm 13	1 \pm 1	25 \pm 4	4 \pm 1
TXNDC1	Thioredoxin domain-containing protein 1	63 \pm 9	0 \pm 0	31 \pm 5	2 \pm 1
MTDH	Metadherin/LYRIC	45 \pm 8	0 \pm 0	42 \pm 4	1 \pm 1
CD3D	T-cell surface glycoprotein CD3 delta chain	29 \pm 7	0 \pm 0	48 \pm 14	1 \pm 1
SCAMP3	Uncharacterized protein SCAMP3	21 \pm 3	3 \pm 1	58 \pm 28	4 \pm 0
SNAP23	Synaptosomal-associated protein 23	25 \pm 3	2 \pm 1	44 \pm 16	0 \pm 0
RAP2B	Ras-related protein Rap-2b	37 \pm 3	0 \pm 0	26 \pm 4	0 \pm 0
GNAQ	Guanine nucleotide binding protein q subunit	38 \pm 8	0 \pm 0	23 \pm 2	0 \pm 0
KIAA0152	Uncharacterized protein KIAA0152	34 \pm 8	0 \pm 0	21 \pm 4	0 \pm 0
PI4K2A	Phosphatidylinositol 4-kinase type 2-alpha	30 \pm 4	0 \pm 0	20 \pm 2	0 \pm 0
RAP2C	Ras-related protein Rap-2c	34 \pm 2	0 \pm 0	12 \pm 2	0 \pm 0
FLOT1	Flotillin-1	24 \pm 5	0 \pm 0	19 \pm 4	0 \pm 0
RAP2A	Ras-related protein Rap-2a	22 \pm 2	0 \pm 0	9 \pm 2	0 \pm 0
SYBL1	Synaptobrevin-like protein 1	12 \pm 1	0 \pm 0	18 \pm 4	0 \pm 0
GNA13	Guanine nucleotide-binding protein alpha-13 subunit	18 \pm 3	0 \pm 0	9 \pm 1	0 \pm 0
IGSF8 ^a	Immunoglobulin superfamily member 8	11 \pm 1	0 \pm 0	16 \pm 2	0 \pm 0
EBAG9	Placenta-derived apoptotic factor	10 \pm 3	0 \pm 0	17 \pm 2	0 \pm 0
AGPAT1	1-acyl-sn-glycerol-3-phosphate acyltransferase alpha	17 \pm 4	0 \pm 0	8 \pm 2	0 \pm 0
FAM62B	Uncharacterized protein FAM62B	16 \pm 4	0 \pm 0	8 \pm 2	2 \pm 1
FAM108B1	Uncharacterized abhydrolase domain-containing protein	15 \pm 1	0 \pm 0	10 \pm 2	0 \pm 0
VANGL1	Vang-like protein 1	13 \pm 1	0 \pm 0	11 \pm 1	0 \pm 0
SCAMP2	Secretory carrier-associated membrane protein 2	8 \pm 1	0 \pm 0	16 \pm 1	0 \pm 0
LNPEP	Isoform 1 of leucyl-cystinyl aminopeptidase	15 \pm 3	0 \pm 0	7 \pm 3	0 \pm 0
BAT5	Uncharacterized abhydrolase domain-containing protein	11 \pm 2	0 \pm 0	11 \pm 3	0 \pm 0
STX12	Syntaxin-12	10 \pm 2	0 \pm 0	13 \pm 1	0 \pm 0
SCAMP1	Secretory carrier-associated membrane protein 1	9 \pm 1	0 \pm 0	10 \pm 2	0 \pm 0
RHBDD2	Rhomboid domain-containing protein 2	14 \pm 4	0 \pm 0	3 \pm 1	0 \pm 0
HMOX2	Heme oxygenase 2	9 \pm 1	0 \pm 0	9 \pm 1	0 \pm 0
HADHB	Trifunctional enzyme beta subunit	11 \pm 2	0 \pm 0	7 \pm 1	0 \pm 0
GNA11	Guanine nucleotide-binding protein subunit alpha-11	14 \pm 2	0 \pm 0	4 \pm 3	0 \pm 0
STX8	Syntaxin-8	9 \pm 2	0 \pm 0	9 \pm 3	0 \pm 0
ZDHHC20	Probable palmitoyltransferase ZDHHC20	5 \pm 1	0 \pm 0	14 \pm 6	0 \pm 0
SLC1A5	Neutral amino acid transporter B	10 \pm 2	1 \pm 1	7 \pm 2	0 \pm 0

Proteins are listed according to highest total spectral counts identified in both experiment 1 and experiment 2, which compare 17-ODYA-labeled membrane particulate proteomes to palmitic acid-treated and hydroxylamine-treated controls, respectively. Spectral count data represent average values \pm s.e.m.

^aProteins with a consensus myristoylation site (N-Met-Gly).

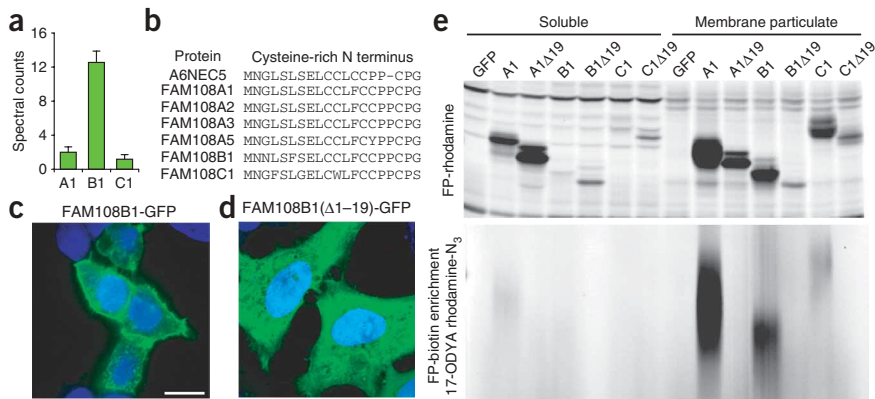


Figure 2 | Membrane tethering of the FAM108 family of serine hydrolases by palmitoylation of an N-terminal cysteine-rich motif. **(a)** Average spectral counts (\pm s.e.m.) of three FAM108 proteins (A1, B1 and C1) identified by 17-ODYA profiling of Jurkat T cells. None of these proteins showed any spectral counts in either the palmitate or hydroxylamine controls (**Supplementary Tables 1 and 2**). **(b)** Cysteine-rich amino acid motif conserved among the seven members of the FAM108 family of proteins. FAM108A3 and FAM108A5 (which were not identified in this study) contain an additional N-terminal sequence preceding the cysteine-rich region of 73 and 28 amino acids, respectively. **(c,d)** Distribution of the FAM108B1-GFP **(c)** and N-terminal truncation mutant FAM108B1(Δ 1–19)-GFP **(d)** fusion proteins (green) expressed in HeLa cells co-stained with DAPI (blue). Scale bar, 15 μ m. **(e)** Fluorophosphonate (FP)-rhodamine-labeled soluble and membrane particulate fractions analyzed by SDS-PAGE and in-gel fluorescence scanning (top). The distribution of active FAM108 protein is shifted from the particulate to soluble fractions by deletion of the N-terminal cysteine rich motif. N-terminal truncations are labeled as A1 Δ 19, B1 Δ 19 and C1 Δ 19 for the truncation mutants of FAM108A1, FAM108B1 and FAM108C1, respectively. GFP is included as a control for transfection. The 17-ODYA-labeled transfected 293T cells were treated with fluorophosphonate (FP)-biotin and enriched with streptavidin-agarose beads, reacted with rhodamine-azide and visualized by SDS-PAGE in-gel fluorescence scanning (bottom).

Many of the predicted palmitoylated proteins are homologs of known palmitoylated proteins characterized in yeast, including 12 members of the multi-transmembrane solute carrier family of transporters, 8 SNAP and NSF attachment receptors (SNAREs) and many metabolic enzymes². The palmitoyl acyl-transferases DHHC5, DHHC6, DHHC20 and HIP14 were also identified as targets of acylation, signifying either auto-palmitoylation or capture of palmitate-loaded catalytic intermediates. We also identified several known T cell-specific targets of palmitoylation, including CD3, CD4, LAT and LCK. In addition to these previously verified palmitoylated proteins, our dataset contained many proteins for which no previous link to palmitoylation has been made.

Any large-scale mass spectrometry-based profiling method is susceptible to generating false positive data, which can become particularly problematic for interpretation of lower-abundance signals. Accordingly, we established a robust protocol to quickly validate proteins enriched in 17-ODYA-treated samples. This method takes advantage of the fact that 17-ODYA-labeled proteins can be visualized by one of multiple platforms, including gel-based readouts (by click chemistry conjugation to rhodamine-azide), which is much simpler and higher-throughput than liquid chromatography-mass spectrometry (LC-MS). We overexpressed 12 high-confidence and 6 medium-confidence targets in 293T cells as fusion proteins tagged with Flag tags and verified their expression western blotting with an antibody to the Flag tag. We directly labeled membrane lysates of the 17-ODYA-labeled cells with rhodamine-azide and analyzed them by SDS-PAGE (see **Supplementary Fig. 4** online for results for a representative 15 of these 18 proteins). Of the 18 proteins analyzed, only 2 (PTBP1 and SHMT2) did not show any

evidence of palmitoylation in 293T cells. Thus, we validated \sim 90% (16/18) of this set of acylation targets, including 11 of 12 high confidence hits and 5 of 6 medium-confidence hits, suggesting that our LC-MS profiles contain a low overall false positive rate. The validated group also contained several potential N-myristoylation targets, including C11orf59, IGSF8, MREG and PAFAH2, based on the presence of an N-terminal Met-Gly sequence. PAFAH2 is a characterized target of myristoylation¹¹ and had a hydroxylamine-resistant fluorescent band, as did C11orf59 (**Supplementary Fig. 4**). The other putative myristoylated proteins showed either complete or near-complete loss in signal after hydroxylamine treatment, suggesting that they are not myristoylated. These results argue that 17-ODYA can also be incorporated into endogenous sites of N-myristoylation. As N-myristoyl-transferases have exquisite selectivity for acyl chains with less than 16 carbon atoms¹², we interpret our data to indicate that N-myristoylated proteins are likely labeled by metabolic products of 17-ODYA fatty acid oxidation, which is presumably the major route of probe degradation.

Included in our dataset were three members of a group of seven highly conserved ($>$ 70%), uncharacterized human serine hydrolases, termed FAM108 proteins (**Fig. 2a** and **Supplementary Fig. 5** online). We have previously shown these enzymes are exclusively found in the membrane fraction of the mouse brain proteome, where we had detected their activity by activity-based protein profiling with serine hydrolase-reactive fluorophosphonate probes¹³, such as fluorophosphonate-biotin and fluorophosphonate-rhodamine¹⁴. Notably, none of the FAM108 enzymes have predicted transmembrane domains, suggesting that their exclusive presence in membrane proteomes is due to a distinct mechanism. Our data raised the possibility that these enzymes associate with the membrane via palmitoylation. The FAM108 protein family shares a highly conserved N-terminal cluster of 4–5 cysteines, which are candidate sites of palmitoylation (**Fig. 2b**). Consistent with this premise, C-terminal GFP fusion revealed striking plasma membrane localization for FAM108 proteins (**Fig. 2c** and **Supplementary Fig. 5**), which was eliminated by deletion of the N-terminal cysteine cluster (**Fig. 2d**). This truncation did not appear to impair enzyme activity, as each enzyme still reacted with fluorophosphonate-rhodamine. In contrast, N-terminally truncated FAM108 enzymes showed a complete loss of palmitoylation signals as judged by 17-ODYA labeling and a clear shift in subcellular distribution from the membrane/particulate to soluble proteome (**Fig. 2e**). Notably, FAM108C1, which contains one less N-terminal cysteine, exhibited markedly less 17-ODYA labeling and was more diffusely distributed and enriched on internal membranes (**Supplementary Fig. 5**). This finding suggests that multiple cysteines near the N termini of FAM108 proteins are palmitoylated, and the extent of palmitoylation could dictate the subcellular localization of these enzymes.

Understanding the complexities of protein acylation remains a major challenge. Here we report to our knowledge the first global inventory of acylated proteins from human cells using a bioorthogonal labeling strategy for the enrichment and identification of palmitoylated proteins. We also provide a technically straightforward gel-based method to rapidly validate palmitoylated proteins identified by large-scale proteomic screens. Future efforts to directly identify sites of palmitoylation may be possible, but our initial efforts to achieve this goal suggest that adjusted protocols will be required to preserve the labile thioester linkage throughout the analysis. Global proteomic analysis will be essential to identify the specific targets of individual palmitoyl acyl transferases and thioesterases, and their related (patho)physiological functions. In contrast to static measurements such as ABE, metabolic labeling with 17-ODYA can potentially allow for a more straightforward assessment of dynamic palmitoylation, by, for instance, following the timecourse of acylation. Furthermore, given the literature precedent of using 17-ODYA *in vivo*¹⁵, this probe may prove useful for profiling palmitoylation events in a range of organisms, including mammals.

Note: Supplementary information is available on the Nature Methods website.

ACKNOWLEDGMENTS

We thank E. Weerapana (The Scripps Research Institute) for providing reagents and assistance with click chemistry and mass spectrometry, G. Simon for assistance

with data analysis, W. Kiossis for microscopy instruction and members of the Cravatt laboratory for helpful discussions. This research was funded by F32NS060559, CA087660 and the Skaggs Institute for Chemical Biology.

AUTHOR CONTRIBUTIONS

B.R.M. performed experiments. B.R.M. and B.F.C. designed experiments, analyzed data and wrote the paper.

Published online at <http://www.nature.com/naturemethods/>
Reprints and permissions information is available online at
<http://npg.nature.com/reprintsandpermissions/>

- Linder, M.E. & Deschenes, R.J. *Nat. Rev. Mol. Cell Biol.* **8**, 74–84 (2007).
- Roth, A.F. *et al. Cell* **125**, 1003–1013 (2006).
- Hang, H.C. *et al. J. Am. Chem. Soc.* **129**, 2744–2745 (2007).
- Heal, W.P., Wickramasinghe, S.R., Leatherbarrow, R.J. & Tate, E.W. *Org. Biomol. Chem.* **6**, 2308–2315 (2008).
- Kostiuk, M.A. *et al. FASEB J.* **22**, 721–732 (2008).
- Martin, D.D. *et al. FASEB J.* **22**, 797–806 (2008).
- Shak, S., Reich, N.O., Goldstein, I.M. & Ortiz de Montellano, P.R. *J. Biol. Chem.* **260**, 13023–13028 (1985).
- Speers, A.E. & Cravatt, B.F. *Chem. Biol.* **11**, 535–546 (2004).
- Link, A.J. *et al. Nat. Biotechnol.* **17**, 676–682 (1999).
- Old, W.M. *et al. Mol. Cell. Proteomics* **4**, 1487–1502 (2005).
- Matsuzawa, A. *et al. J. Biol. Chem.* **272**, 32315–32320 (1997).
- Towler, D.A. *et al. J. Biol. Chem.* **263**, 1784–1790 (1988).
- Blankman, J.L., Simon, G.M. & Cravatt, B.F. *Chem. Biol.* **14**, 1347–1356 (2007).
- Liu, Y., Patricelli, M.P. & Cravatt, B.F. *Proc. Natl. Acad. Sci. USA* **96**, 14694–14699 (1999).
- Gebremedhin, D. *et al. J. Vasc. Res.* **30**, 53–60 (1993).